Pergamon

PII: S0277-5387(97)00391-4

Polyhedron Vol. 17, No. 8, pp. 1295–1301, 1998

0277–5387/98 $19.00+0.00

2-D COSY and NOESY ^{1}H NMR spectral studies on pyrazine-bridged dizinc(II)diporphyrin complex

Stanisław Wołowiec*

Department of Chemistry, University of Wrocław 14 Joliot-Curie 14, 50-383 Wrocław, Poland

(Received 5 June 1997; accepted 26 August 1997)

Abstract—The dinuclear [Zn(TTP-*m*-O-(CH_2)–)]$_2(CH_2)$ complex **1** (where TTP-*m*-O = 5-(*meta*-hydroxyphenyl)-10,15,20-tritolylporphyrin dianion) coordinates axially nitrogen bases; pyrazine (Py) and pyrimidine. The solid 1 : 1 Py : **1** adduct has been isolated and identified as dinuclear complex (μ-Py) [Zn(TTP-*m*-O-$(CH_2)-]_2(CH_2)$ **2** with pyrazine base bridging intramolecularly two zinc(II) metal ions based upon variable temperature 1-D and 2-D ^{1}H NMR spectral measurements.

Keywords: dizinc(II)diporphyrin; pyrazine bridging; 2-D ^{1}H NMR spectroscopy.

In the previous papers of the series, dealing with dinuclear complexes of diporphyrins linked via flexible spacer, the coordination properties of diiron(III) and iron(III)/copper(II) diporphyrins with cyanide in organic solvents have been studied [1,2]. It has been found that the two proximal metal ions promote the formation of μ-cyanide dinuclear complexes in CN^--deficient solutions.

The dimetallic complexes of diporphyrins were studied extensively from the viewpoint of their catalytic activity [1,2] and references cited therein. The dicobalt(II) and dicopper(II) complexes of diporphyrins with flexible polyhydrocarbon spacer attached to the *meso*-phenyl ring of porphyrin showed high catalytic activity in two-electron oxidation of 3,5-di-*t*-butyl catechol with dioxygen in contrast to mononuclear porphynatocobalt(II) complexes [3]. The coordination of nitrogen bases to dizinc(II) complexes of *meso*-(tetraryl)porphyrin-based diporphyrins with the polyhydrocarbon spacer of variable length attached to *ortho*-, *meta*-, or *para*- *meso*-phenyl were studied in detail [3,4]. It has been found that the dizinc(II) complex of diporphyrin with a three-carbon spacer attached to *ortho*-phenyl Zn^{II}TTP*o*-O$(CH_2)_3$O-*o*TPPZn^{II}, coordinated two molecules of lutidine with $K_1/K_2 = 160$ while for its analogue Zn^{II}TTP*p*-O$(CH_2)_3$O-*p*TTPZn^{II} the ratio $K_1/K_2 = 1$. The low value of K_2 for the former is due to the steric hindrance from the second *ortho*-appended Zn(II)porphyrin half, which makes one face of Zn(II)porphyrin moiety less accessible for coordination of the second monodentate axial nitrogen base [4]. When a suitable heteroaromatic base with two nitrogen atoms (1,*n*-bis(4-pyridyl)alkane, where $n = 0$, 2, or 3) was applied as a ligand for dizinc(II) complex with face–face diporphyrin, with two diamido-type spacers attached to *ortho*- position of 5,15-*meso*-phenyls, and strapped on the opposite porphyrin face by another diamido substituent attached to 10,20-*meso*-phenyls, the intramolecular bridging of the nitrogen base was found to be dependent on the geometric factors of the studied systems [5]. In those rigid host–guest systems the best tuning between interporphyrin distance and the length of guest was achieved in the case of phenylenediamido spacer and 4,4′-bipyridyl as a guest [5]. The affinity of 4,4′-bipyridyl and other nitrogen bases to coordinate to zinc(II)porphyrin has been utilized in ligand-templated synthesis of cyclic and linear porphyrin oligomers [6,7]. A number of papers have been published in which di- and oligoporphyrins were assembled to study the energy transfer and photoinduced electron transfer in dizinc(II)diporphyrins adjacent together by means of coordinated, bridging axial nitrogen base [8,9].

Here the spontaneous conformational adjustment between the dizinc(II) diporphyrin with single, flexible spacer adjacent into *meso*-aryl substituents on both

* E-mail: sw@wchuwr.chem.uni.wroc.pl

porphyrin halves and pyrazine (and not pyrimidine) led to the isolation of pyrazine:Zn^{II}TTP*m*-O$(CH_2)_3$O-*m*TPPZn^{II} 1:1 adduct. The complex was studied by means of the ^{1}H NMR 2D COSY and NOESY spectral methods.

EXPERIMENTAL

Syntheses

Synthesis of [Zn(TPP-*m*-O-(CH_2)–)]$_2(CH_2)$ (**1**). The diporphyrin (H_2TTP-*m*-O-$(CH_2)_3$-O-*m*-$TPPH_2$) was synthesized according to the modified method of Little [10,1]. Zinc(II) ion was inserted by dropwise addition of 20-fold excess of zinc(II) chloride in methanol into the chloroform solution of (H_2TTP-*m*-O-$(CH_2)_3$-*O*-*m*-$TPPH_2$) under reflux in the presence of solid zinc(II) carbonate. The complex was separated chromatographically from impurities and solid materials on basic alumina (methylene dichloride eluent).

^{1}H NMR (the assignments based on ^{1}H 2D COSY and NOESY experiments, for numbering see Scheme 1): 8.90 ppm (8H, AB system, J_{AB} = 4.8 Hz, δ_A = 8.91 ppm, δ_B = 8.89 ppm, pyrrole β-H, 12,13(17,18)), 8.87 ppm (8H, AB system, J_{AB} = 4.8 Hz, δ_A = 8.90 ppm, δ_B = 8.85 ppm, pyrrole β-H, 2,3(7,8)), 8.05 ppm (4H, doublet, J_{om} = 7.9 Hz, o_3+o_4), 8.00 ppm (4H, doublet, J_{om} = 7.9 Hz, o_1), 7.96 ppm (4H, doublet, J_{om} = 7.9 Hz, o_2), 7.74 ppm (2H, singlet, o_6), 7.73 ppm (2H, doublet, J_{om} = 7.2 Hz, o_5), 7.53 ppm, (2H, doublet of doublets, J_{om} = 7.2 Hz, J_{mp} = 7.7 Hz, m_5), 7.50 ppm (4H, doublet, J_{om} = 7.9 Hz, m_3+m_4) 7.43 ppm (4H, doublet, J_{om} = 7.9 Hz, m_1), 7.39 ppm (4H, doublet, J_{om} = 7.9 Hz, m_2), 7.26 ppm (2H, doublet, J_{pm} = 7.7 Hz, p), 4.33 ppm (4H, triplet, $J_{\alpha\beta}$ = 6.1 Hz, $CH_{2(\alpha)}$), 2.66 ppm (6H, singlet, methyl at 15-*meso*-phenyl), 2.60 ppm (12H, singlet, methyls at 10- and 20-*meso*-phenyls), 2.36 (2H, quintet, $CH_{2(\beta)}$). UV–Vis (λ[nm], (ε [$mol^{-1} \times dm^3$])): 423 (6.57×10^6); 552 (1.24×10^5); 594 (1.15×10^5).

Synthesis of (Py){[Zn(TTP-*m*-O-(CH_2)–)]$_2(CH_2)$} (**2**) Equimolar amounts of **1** and pyrazine were dissolved in chloroform (0.2 M) and hexane was carefully layered over the chloroform solution. The mixture was left for slow codiffusion of solvents at 0°C. Large, purple crystals were formed after 2 days. The crystals contained three molecules of solvent per one molecule of (Py){[Zn(TTP-*m*-O-(CH_2)–)]$_2(CH_2)$} (determined by integration of resonances in the ^{1}H NMR spectrum of $2 \times 3CHCl_3$). The crystals were too fragile to be mounted in X-ray diffractometer and therefore the weakly bound chloroform molecules were removed from the solid by a high vacuum applied overnight to the isolated crystals. Inspection of the ^{1}H NMR spectrum indicated that solvent molecules were no longer present. The crystals turned into powder after evaporation of the solvent.

Methods and reagents

^{1}H NMR spectra were obtained with a Bruker AMX300 spectrometer operating in the quadrature mode at 300 MHz. The 2-D COSY and NOESY spectra were collected by use of 1024 points in t_2 over desired bandwidth and 512 t_1 blocks with 16 scans per block in which four dummy scans were included. Repetition time was 2 s in all cases, the mixing time was 0.6 s for NOESY measurements. The NOESY spectra were processed in the phase-sensitive or magnitude modes. The deuterated solvents used were obtained from Glaser AG. The residual chloroform peak at 7.24 ppm was used as the internal chemical shift standard in presented spectra. The UV–Vis spectra were taken with HP 8453 diode-array spectrophotometer.

The equilibrium constant for the reaction:

$$Zn/Zn + py \rightleftharpoons Zn(\mu\text{-py})Zn$$

has been determined by both UV–Vis and ^{1}H NMR spectral titration at 295 K.

In the UV–Vis titration procedure 4.2×10^{-6} M solution of **1** in chloroform has been titrated with pyrazine stock solutions to achieve variable concentration of pyrazine within $2.15 \times 10^{-6} \div 0.2$ M region. A slight shift of Soret band into 422 nm and red shift of the Q-bands into 560 and 600 nm upon pyrazine coordination were found. Well resolved isosbestic points at 557 and 598 nm in the region of Q-bands up to 9.4×10^{-3} M pyrazine concentration were observed. The UV–Vis data were worked up at two wavelengths: 552 nm (corresponding to starting complex **1**) and 600 nm (corresponding to the maximum of the pyrazine adduct). Putting the two-parameter fitting procedure (equilibrium constant K and absorbance of the pyrazine adduct A_∞) into the equation:

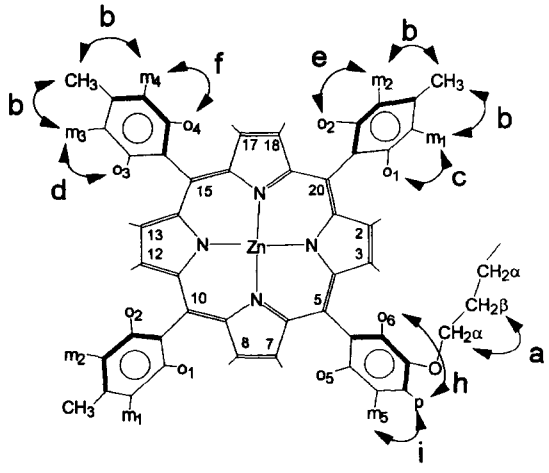

Scheme 1.

$$K = \frac{(A - A_0)}{(A_0 - A_\infty) \cdot [\text{py}]}$$

gave the averaged value of $K = 2.0(\pm 0.3) \times 10^4\ \text{M}^{-1}$.

In the ^{1}H NMR titration, 0.0038 M solution of **1** in $CDCl_3$ has been titrated with 0.2 M stock solution of pyrazine using the microsyringe technique. The pyrrole β-H resonances shifted from 8.93 ppm (δ_f) into 8.58 ppm (δ_c, the final chemical shift achievable upon the increase of pyrazine concentration above 0.005 M). The pairs of data, observed averaged chemical shift vs total pyrazine concentration, were fitted into the equation obtained by combination of the equations:

$$\delta = \delta_f \cdot p_f + \delta_c \cdot p_c,$$

where p_f and p_c are the populations (molar contributions) of free and pyrazine-coordinated dizinc(II)diporphyrin, respectively, and δ is observed chemical shift in titration procedure,

$$p_f + p_c = 1, K = \frac{p_c}{p_f \cdot [\text{py}]_f}$$

where $[\text{py}]_f$ is the concentration of free pyrazine. The solution of the resulting quadratic equation leads to the final relationship:

$$\delta = \frac{(\delta_f - \delta_c) \cdot \{C_0 \cdot \text{K} - [\text{py}]_0 \cdot \text{K}}{2 \cdot \text{C}_0 \cdot \text{K}} + \\ + \frac{\sqrt{[(1 + [\text{py}]_0 \cdot \text{K} - \text{C}_0 \cdot \text{K})2 + 4 \cdot \text{C}_0 \cdot \text{K}]}\}}{2 \cdot \text{C}_0 \cdot \text{K}} + \delta_c$$

where C_0 = the concentration of **1** and $[\text{py}]_0$ = the total concentration of pyrazine.

One-parameter fitting procedure resulted in the value of $K = 1.2(\pm 0.5) \times 10^4\ \text{M}^{-1}$.

Molecular mechanics calculations using the HyperChem software (Autodesk) were carried out and displayed on a PC 486 computer. The standard MM+ force field, with the constrains set on coordination bonds to achieve the geometry around the zinc(II) central ion were adapted from the published X-ray crystallographic data on pentacoordinate pyridine Zn(II)porphyrin complexes [11,12].

RESULTS AND DISCUSSION

The 1-D ^{1}H NMR *spectral results on coordination of pyrazine and pyrimidine to* **1**

Previously we have examined the ^{1}H NMR spectra of (H_2TTP-*x*-O-$(CH_2)_n$-O-*x*-TPPH_2) diporphyrin (n = 2,3, x = *o*-, *m*-, and *p*-) in detail [1]. In case of *ortho*-appended diporphyrins the ring current originated from neighbouring porphyrin macrocycle induced large upfield shifts of spacer-attached phenyl ring protons. It was not the case for the diporphyrin used here and consequently all resonances from aromatic *meso*-phenyls were grouped within the region of: 8.08–7.76 ppm (*ortho*); 7.58–7.40 ppm (*meta*); and 7.30 ppm (*para*). Nevertheless, the asymmetry imposed by one different *meso*-substituent (5-*meso*-substituted phenyl versus three *p*-methylphenyls) resulted in non-equivalence of β-pyrrole resonances, which gave one AB spectrum (2,3(7,8)) and a singlet (12,13(17,18)). Also, the presence of large aromatic porphyrin macrocycle appended at the *meta* position of *meso*-phenyl induced substantial up and down non-equivalence of *ortho* and *meta* 10- and 20-*meso*-phenyl protons. Both of these tendencies are even more pronounced in the case of dizinc(II) complex **1**, where all the β-pyrrole rings bear non-equivalent pairs of protons (two AB spectra, see Experimental).

The coordination of heteroaromatic bases: pyrazine and pyrimidine has been monitored by titration of **1** with these ligands. It was found that the system was in fast exchange on the ^{1}H NMR timescale. The chemical shift of ligands was always ligand concentration dependent. However, the isolation of solid **2** of fixed stoichiometry (1 : 1 of **1** : pyrazine) indicated that the complex of that stoichiometry is particularly stable in solid state. The crystal structure of **2** was not available. Thus it was necessary to find the method to determine if pyrazine bridges two Zn(II) intra- or intermolecularly in **2**. Neither mass spectrometric nor osmometric measurement results gave a definite answer to that question, due to the fast exchange between free and coordinated axial ligand processes taking place in solution **2**. However, an inspection of the ^{1}H NMR spectra showed that the chemical shift of **2** measured at three different solvents (chloroform, methylene dichloride and toluene), at four different temperatures (between 190 and 273 K), was only slightly dependent on concentration of **2**. Considering the possible routes leading to the formation of intramolecularly bridged dizinc(II) species (sequence of reactions (1) and (2)) and an intermolecularly bridged complex (sequence of reactions (1), (3), and (4)):

$$\text{Zn/Zn} + \text{py} \rightleftharpoons \text{pyZn/Zn} \quad (1)$$

$$\text{pyZn/Zn} \rightleftharpoons \text{Zn}(\mu\text{-py})\text{Zn} \quad (2)$$

$$\text{pyZn/Zn} + \text{py} \rightleftharpoons \text{pyZn/Znpy} \quad (3)$$

$$2\text{pyZn/Znpy} \rightleftharpoons \{\text{pyZn/Znpy})\}_2 \quad (4)$$

where Zn/Zn represents the starting complex **1**, pyZn/Zn corresponds to the species containing monodentate coordinate pyrazine, Zn(μ-py)Zn represents intramolecularly bridged dinuclear complex, pyZn/Znpy corresponds to the dinuclear complex containing two pyrazine coordinated via one nitrogen donor, and $\{\text{pyZn/Znpy})\}_2$ represents tetranuclear species with two pyrazine ligands bridging two dizinc(II)diporphyrin molecules), one may expect that in the case of intermolecular bridging, the chemical shift of pyrazine resonance or any porphyrin proton (the o_6 resonance was monitored as the most sensitive to pyrazine coordination) should substantially depend on [2] due to associative character of reaction (4). In

fact, within the concentration range used (0.01–0.5 M) the chemical shift of both pyrazine and o_6 protons are almost independent of concentration of **2**. Thus, it was assumed that **2** is a dizinc(II) complex bridged intramolecularly with pyrazine ligand. This conclusion was then strongly supported by the fact that when pyrimidine was used instead of pyrazine, the ligand resonances were considerably less shifted upon coordination if compared to **2**. The coordination shift in the latter case was comparable with that for TTPZn(II) mononuclear analogue (Table 1). The downfield coordination shift of 2-H of axial ligand (pyrmidine and pyridine), due to porphyrin ring current effect, was comparable (4.2 and 4.9 ppm, respectively) in both cases, suggesting the monodentate binding mode of pyrmidine into **1**. Intramolecular bridging of two zinc(II) centres of pyrazine in **2** leads to a larger coordination shift ($\Delta = 7.9$ ppm) due to additive ring current shifts from two porphyrin macrocycles.

The estimation of the equilibrium constant for the reaction of the formation of **2** (reactions (1)+(2)) based on UV–Vis and ^{1}H NMR spectral titrations gave the values 2.0 ($\pm$0.3) $\times 10^4$ and 1.2 ($\pm$0.5) $\times 10^4$ M^{-1}, respectively, which are in fair agreement despite the fact that three orders of magnitude of different concentrations were used in those two experiments. The value of log K = 4.3 found for **1** is larger than that for binding of pyridine or bipyridyl to monomeric zinc(II)porphyrins and comparable to those found for bridging coordination to rigid dizinc(II)diporphyrins which are not well-suited to adopt the ligand due to steric reasons [5,6]. In some cases of face-to-face dizinc(II)diporphyrins the cooperative coordination led to log K as large as 7.4 [5] and 8.8 [6]. Here the cooperative effect is not large due to the fact that two porphyrins are adjacent together with flexible spacer.

The ^{1}H NMR spectrum of **2** in chloroform at room temperature consists of broad resonances both from the phenyl ring of diporphyrin macrocycle and from the pyrazine ligand. The spectrum changes remarkably at lower temperatures (Fig. 1). The pyrazine res-

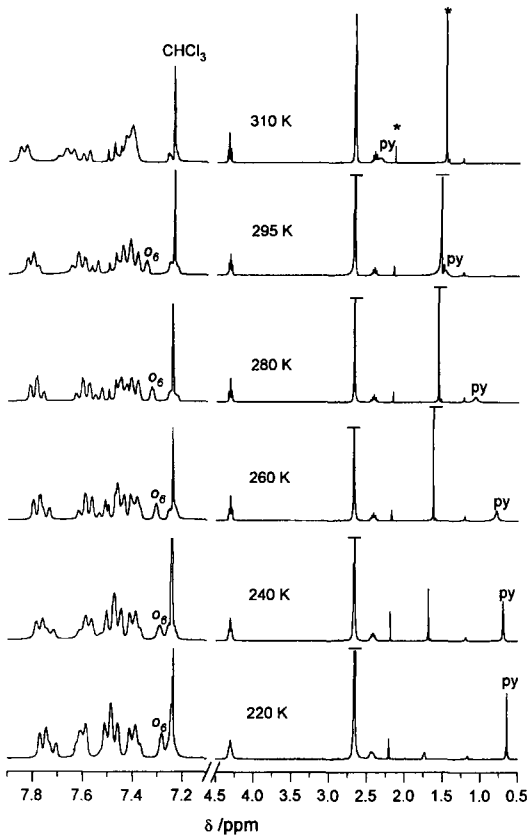

Fig. 1. The variable temperature ^{1}H NMR spectra of **2** in chloroform-*d*. The pyrazine hydrogen resonance is labelled as py, the impurity and residual water at 1.75 ppm resonances are labelled with asterisk.

Table 1. The ^{1}H NMR chemical shifts δ and coordination shift Δ (in parentheses) of pyrazine and pyrimidine protons for free and coordinated ligands (measured for 0.04 M $CDCl_3$ solutions)

	Temperature	pyrimidine			pyrazine
Composition of solution	[K]	δ 2 (Δ)	δ 4,6 (Δ)	δ 5 (Δ)	δ (Δ)
	295	9.2	9.71	7.3	8.6
	220	9.2	8.74	7.4	8.6
1 : *1* **1** : pyrimidine	310	6.25	6.82	6.37	
	295	5.76	6.51	6.23	
	280	5.37	6.27	6.13	
	260	4.98	6.04	6.04	
	240	4.83	6.03	5.91	
	220	4.80 (4.2)	6.05 (2.7)	5.90 (1.3)	
1 : *1* **1** TTPZn(II) : pyrazine	220				3.67 (4.93)
2	220				0.69 (7.91)

onance shifts 1.7 ppm upfield upon lowering temperature by 90° and further temperature decrease (down to 180 K in methylene dichloride-d_2 solvent) does not cause either the chemical shift changes or splitting of pyrazine or aliphatic resonances. Obviously, even in methylene dichloride solvent, at 180 K the rotation of pyrazine ligand around coordination bonds remains fast on NMR scale. Simultaneously the resonances from aliphatic spacer broaden and some changes are observed within an aromatic region of spectrum. Total assignment of resonances of **2** could provide some detailed information on the molecular structure of **2**. Therefore, 2-D ^{1}H NMR measurements were performed, particularly to analyze the crowded aromatic part of the ^{1}H NMR spectrum. The standard 2D ^{1}H NMR COSY and NOESY methods were used.

The total assignments of ^{1}H NMR *resonances based on* 2-D COSY *and* NOESY *results*

At 280 K the aromatic resonances in the region of 7–8 ppm are sharp and well-resolved and the COSY experiment allows to assign the resonances of *meso*-phenyls. The COSY map is presented in Fig. 2(A) and (B). The cross-peak **a** between α and β methylene protons of spacer was obvious and the cross-peak **b** between *p*-methylphenyl protons and the protons in aromatic region (Fig. 2(A)) allowed to identify the *meta*-phenyl proton resonances and provided a suitable starting point to analyze the cross-peaks within the aromatic region (Fig. 2(B)). Thus, two overlapping doublets of doublets of the relative intensity 2 : 1 at 7.8 ppm were assigned to the *ortho*-protons o_1 and o_3 (see the connectivity pattern at Scheme 1) located at the opposite side of porphyrin macrocycle plane to the appended second porphyrin ring. They were combined with the *meta* protons m_1 and m_3 via cross-peaks **c** and **d** (Fig. 2(B)). Two overlapping doublets of doublets of relative intensity 1 : 2 centred at 7.6 ppm belong to o_4 and o_2 protons, respectively and were coupled with the m_4 and m_2 resonances via cross-peaks **f** and **e**, respectively. It was assumed that *ortho* protons located at the same side of porphyrin plane as appended porphyrin ring (o_2 and o_4) should resonate at higher fields than o_1 and o_3. Corresponding pairs of *otho* protons are weakly coupled (cross-peak **g**). The 5-*meso*-phenyl ring protons gave the cross-peak pattern consistent with the couplings between *para* proton (overlapped with chloroform residual resonance at 7.24 ppm) and *meta* proton (triplet centred at 7.50 ppm at this temperature) by cross-peak **i** and *ortho*- proton o_6 located at the appended porphyrin side) by cross-peak **h**. The remaining cross-peak (not marked) corresponds to the vicinal coupling between o_5 (the resonance at 7.55) and m_5. As expected, the magnetic non-equivalence between *ortho* protons at the 5-*meso*-phenyl ring, attached via spacer to the second porphyrin was the largest of all *meso*-phenyls. The resonance of o_6 was the most upfield shifted of all

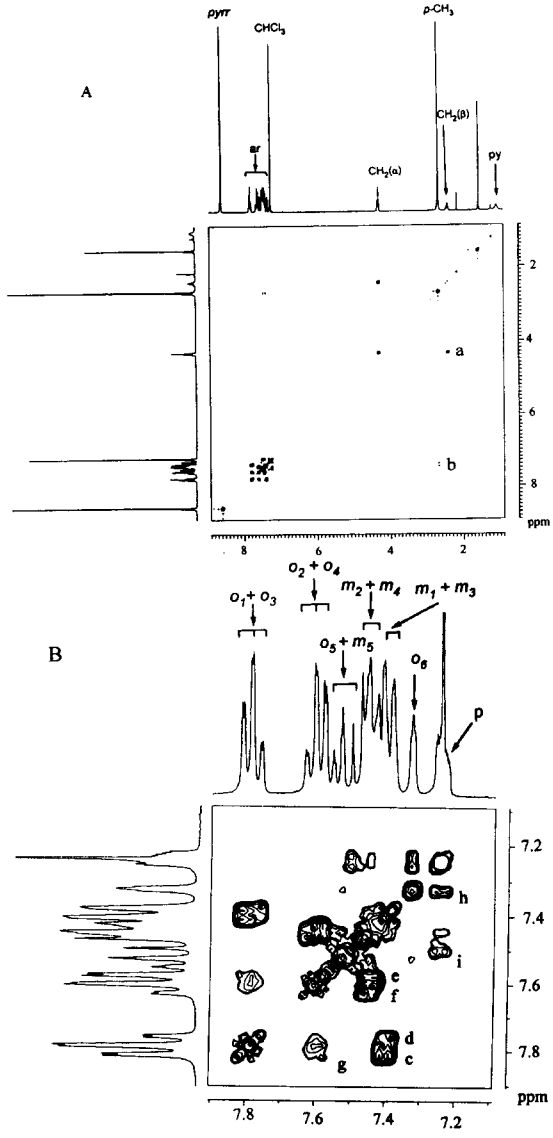

Fig. 2. The COSY map of **2**: (A), full spectrum taken at 280 K; (B), the expanded aromatic region. The abbreviations used are: *pyrr*: β-H pyrrole resonances; ar: the resonances of *meso*-phenyl protons; other labels follow those used in Scheme 1.

aromatic *ortho* and *meta* protons and it was located at a very fortunate position between other aromatic resonances from the downfield side and residual chloroform plus *para* proton resonance from the high-field side.

This connectivity pattern (presented at Scheme 1) was then confirmed by NOE cross-peaks obtained in NOESY experiment performed at 230 K. At this temperature the resonance from pyrazine protons is sharp and that provided a good opportunity to observe the spatial proximity of that proton with the porphyrin protons. The relevant fragments of NOESY map are presented in Fig. 3(A) and (B).

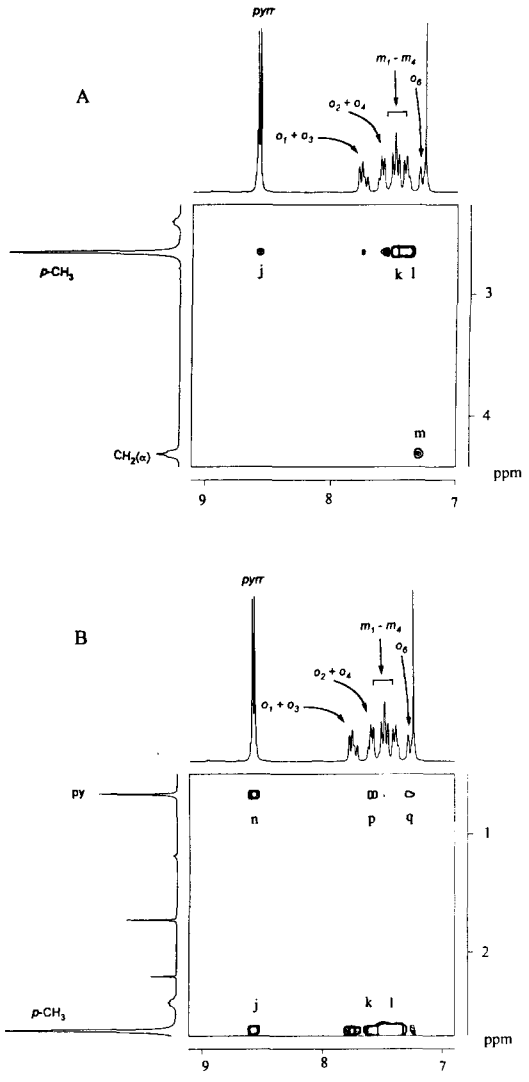

Fig. 3. The relevant fragments of NOESY spectrum of **2** taken at 230 K.

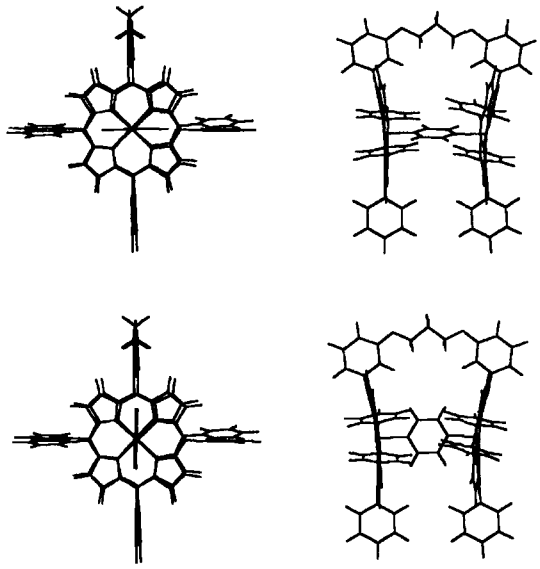

Fig. 4. Two projections of isomer **A** (upper pair) and **B** (lower pair) of **2** as obtained by MM+ calculations (using HyperChem program).

The observed cross-peaks: **j** between β-pyrrole and *p*-methyl protons, cross-peaks **k** and **l** between *p*-methyl and *meta* protons within porphyrin macrocycle were expected. The cross-peak **m** between α-methylene protons and o_6 confirmed the assignment of the latter unambiguously. The NOE cross-peaks **n, p,** and **q** indicated the spatial proximity of pyrazine protons to the β-pyrrole, o_2 o_4, and o_6, respectively (Fig. 3(B)) proving the proper assignment of o_2 and o_4 protons as those located at the same side of porphyrin macrocycle as appended porphyrin and bridging aromatic pyrazine ring.

The conformation of **2** *based on molecular model and* ^{1}H NMR *chemical shift*

In order to analyze details of confirmation of the intramolecularly bridged dinuclear complex the molecular model of **2** was constructed by means of HyperChem program. The set of constraints was imposed, in particular the Zn(II)—N(pyrrole) = 2.06 and Zn(II)—N(axial) = 2.14 Å bond lengths based on mean values taken from crystallographically established structures of pyridine pentacoordinate complexes of Zn(TPyP) and Zn(TPP–C_3Py) [11,12]. The resultant two conformations of **2** are presented in Fig. 4. The bridging pyrazine ring is located in the cavity along the C_{10}–C_{20} in case of rotational isomer **A,** whereas the isomer **B** bears the pyrazine ring rotated 90° along the coordination bonds. Although the free rotation of pyrazine can be reasonably assumed due to observation of NOE effects between pyrazine protons and all *ortho* phenyl protons located at the same side of porphyrin macrocycles as the bridging pyrazine, the analysis of chemical shift changes of *ortho* protons upon coordination indicates that the larger effect reveal o_6 (0.49 ppm upfield at 220 K) and o_4 (0.43 ppm upfield) protons in comparison with o_2 (0.35 ppm upfield). This suggests the larger contribution of rotational isomer **A,** for which the closest through-space contact estimated from molecular model between pyrazine proton and o_2 equals 2.81 Å whereas the distances between pyrazine protons and o_6 and o_4 are 3.16 and 2.91 Å, respectively, in isomer **B.**

Thus the dominating conformation of **2** can be represented by isomer **A** in Fig. 4. The pyrazine-bridged, diamagnetic dizinc(II) diporphyrin complex obtained as crystalline adduct serves a good standard for estimation of the isotropic shift for paramagnetic complexes with bridging pyrazine [13].

REFERENCES

1. Wołowiec, S. and Latos-Grażyński, L., *Inorg Chem.*, 1994, **33,** 3576.
2. Wołowiec, S., *Polyhedron*, 1997, **21**, 3779.
3. Okamoto, M., Oishi, N., Nishida, Y. and Kida, S., *Inorg. Chim. Acta*, 1982, **64,** L217.
4. Krausz, P. and Giannotti, C., *J. Chim. Phys.*, 1983, **80,** 299.
5. Yemori, Y., Nakatsubo, A., Imai, H., Nakagawa, S. and Kyuno, E., *Inorg. Chem.*, 1992, **31,** 5164.
6. Anderson, H. L. and Sanders, J. K. M., *Angew. Chemie Int. Ed. Engl.*, 1990, **29,** 1400.
7. Anderson, S., Anderson, H. L. and Sanders, J. K. M., *Angew. Chemie Int. Ed. Engl.*, 1992, **31,** 907.
8. Imahori, H., Yamada, K., Yoshizawa, E., Hagiwara, K., Okada, T. and Sakata, Y., *J. Porphyrins Phthalocyanines*, 1997, **1,** 55 and references 6–13 cited therein.
9. Vaijayanthimala, G. and Krishnan, V., *J. Porphyrins Phthalocyanines*, 1997, **1,** 17.
10. Little, R. G., *J. Heterocycl. Chem.*, 1978, **15,** 203.
11. Collins, D. M. and Hoard, J. L., *J. Am. Chem. Soc.*, 1970, **92,** 3761.
12. Bobrik, M. A. and Walker, F. A., *Inorg. Chem.*, 1980, **19,** 3383.
13. Wołowiec, S. The data on cyanide and pyrazine mixed ligand complexes of diiron(III)diporphyrin will be presented elsewhere.